Research on Chemical Intermediates (2019) 45:3165–3181
https://doi.org/10.1007/s11164-019-03785-5

Effect of preparation parameters on properties and performance of Pd/Al_2O_3 catalyst in saturation of olefins

Jamaledin Howeizi[1,2] · Saeed Taghvaei-Ganjali[1] · Mercedeh Malekzadeh[1] · Fereshteh Motiee[1] · Saeed Sahebdelfar[2]

Received: 5 November 2018 / Accepted: 22 February 2019 / Published online: 4 March 2019

Abstract

The complete saturation of commercial olefin-containing (3.3 mol%) C_4 stream over $Pd/\gamma\text{-}Al_2O_3$ catalysts was studied. The catalysts were prepared by wet impregnation of the support using acidified $PdCl_2$ solutions. The effect of different preparation parameters such as $HCl/PdCl_2$ ratio in impregnation solution, impregnation time and solution volume on palladium distribution and catalytic performance was investigated. The catalysts were characterized by N_2 adsorption/desorption, ICP measurements, X-ray diffraction, temperature programmed desorption of ammonia (NH_3-TPD) and scanning electron microscopy. Catalytic performance tests were carried out in a three-phase co-current trickle-bed reactor at 50 °C, 27 bar and high olefin conversions in accordance with industrial operating conditions. The catalysts showed different palladium distributions according to preparation procedure. The best performance was observed for egg-shell catalysts prepared by employing short impregnation times (5–10 min) and low competitor levels ($HCl/PdCl_2 = 2.2$ mol mol^{-1}) in impregnation solution. The catalyst lifetime was found to correlate with its activity which was explained by a parallel deactivation mechanism.

✉ Saeed Taghvaei-Ganjali
S_Taghvaei@Iau-tnb.ac.ir

[1] Department of Chemistry, Tehran North Branch, Islamic Azad University, P.O. Box 16511-53311, Tehran, Iran

[2] Catalysis Research Group, Petrochemical Research and Technology Company, National Petrochemical Company, P.O. Box 14358-84711, Tehran, Iran

Graphical abstract

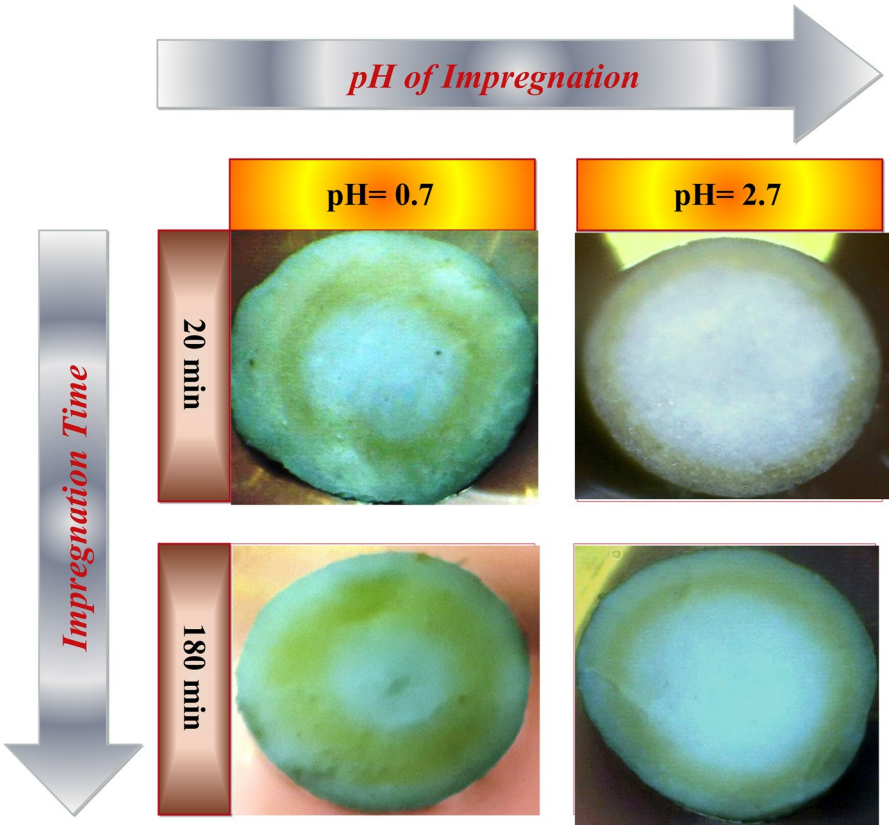

Keywords Complete saturation · Pd/Al_2O_3 catalyst · Impregnation · Pd distribution · Trickle-bed reactor

Introduction

Olefins are important building blocks and feed stocks in chemical industries. However, their presence in paraffinic streams as impurities causes several operational problems because of their high reactivity. These compounds can be eliminated by hydrogenation. The processing of C_3 and C_4 hydrocarbon streams requires a selective hydrogenation process (SHP) and/or a complete saturation process (CSP) unit to remove the olefinic impurities. The full hydrogenation of butadiene to *n*-butane, for instance, may be an opportunity to eliminate surplus diene [1]. The *n*-olefins and diolefins in the feed of isomerization process of MtBE plants are catalyst poisons and they are saturated to butanes (e.g. by Hüls CSP [2, 3]).

$$C_3H_6 + H_2 \rightarrow C_3H_8 \quad (1)$$

$$C_4 \text{ olefins} + H_2 \rightarrow C_4 \text{ paraffins} \quad (2)$$

$$1,3\text{-butadiene} \xrightarrow{H2} n\text{-butenes} \xrightarrow{H2} n\text{-butane} \quad (3)$$

These reactions are exothermic and thermodynamically favorable at low temperatures and higher pressures. Therefore, in practice, low temperatures are employed, which necessitates highly active catalysts.

Simple olefinic and acetylenic compounds are readily hydrogenated in the presence of any typical hydrogenation catalyst [4]. Nickel and palladium are active component of the catalysts in hydrogenation of C–C double bound with palladium being much more active [5]. The palladium is typically dispersed on a high surface area activated alumina support. Owing to its high activity, the catalyst permits operation at low temperatures and high space velocities.

The hydrogenation of alkenes has long been recognized as being structure-insensitive, by which the turn-over frequencies (TOFs) are essentially independent of metallic particle size [6]. In the hydrogenation of olefins over Pd/γ-Al_2O_3 catalysts, two types of active sites are involved, metal sites and acid sites. The metal sites catalyze hydrogenation reactions, but acid sites of the alumina catalyze oligomerization of the olefins, producing heavy residues on the catalyst (green oil), which causes catalyst deactivation [7].

The catalyst is cyclically regenerated by hot hydrogen stripping. The temporary poisons include oxygenates, chlorides (halogens), water, organic nitrogen, caustic, O_2, CO, CO_2 and sulfur compounds. These compounds are eliminated from the feed. Nevertheless, polymerization of the olefinic compounds can cause catalyst deactivation by "coke" formation, especially at high olefin feed concentrations and high temperatures (Scheme 1). This reaction scheme implies a parallel deactivation mechanism [8].

The preparation method strongly influences catalyst performance [9]. Pd/Al_2O_3 catalysts are commonly synthesized by impregnation of the support with $PdCl_2$ solutions. The Pd^{2+} ion favors the formation of square planar PdL_4 complexes [10]. The most commonly utilized negatively charged palladium complex ion is $PdCl_4^{2-}$, which is stable in neutral and acid solutions, provided that the Cl^-/Pd^{2+} ratio is high enough to avoid hydrolysis [11].

Generally, a solution of $PdCl_2$ in diluted hydrochloric acid is used. Cl^- ion acts as a competitive anion in the adsorption of $PdCl_4^{2-}$ and is used for affecting Pd macro-distribution in mm-sized supports. However, the initial metal-ion precursor complex can undergo speciation. Tait et al. [12] studied the speciation of aqueous $PdCl_2$ solutions under acidic and basic conditions using Uv/Vis and Raman spectroscopy. The chloride

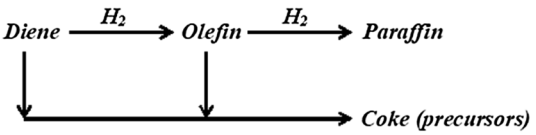

Scheme 1 Simplified reaction path ways in catalytic hydrogenation of olefinic compounds

concentration of the solution was set with NaCl and the pH was set with $HClO_4$, HNO_3 and NaOH. The predominance diagram for Pd(II) chloride species was determined experimentally. It showed that $PdCl_4^{2-}$ is dominant at low pH values and high Cl^- concentrations while mixed Pd-Cl-OH species are dominant in higher pH and lower Cl^- concentrations.

Espinoza-Alosono et al. [13] studied the influence of Cl^- (aq) concentration, solution pH and impregnation time on $PdCl_4^{2-}$ dynamics after impregnation of γ-Al_2O_3 pellets using UV–vis micro-spectroscopy. It was illustrated that, immediately after impregnation, $PdCl_4^{2-}$ is not stable in contact with alumina and undergoes hydrolysis to form $PdCl_{4-x}(OH)_x^{2-}$ species and that Pd complexes appear with different molecular structures depending on pH and equilibration time.

Adsorption of metal complexes on alumina is caused either by electrostatic interactions or by direct chemical reactions [14]. The pH of impregnation solution affects the electric charge on the support surface thereby affecting electrostatic interaction between metal precursor and support. The isoelectric point of alumina is 7.8 [15].

Lomot et al. [16] demonstrated that palladium dispersion strongly depends on the loading. With exactly the same treatment in oxygen and reduction in hydrogen, both at 300 °C, their 1.45 wt% Pd/γ-Al_2O_3 catalyst showed a dispersion of 62%, whereas for the 0.39 wt% catalyst a dispersion of 91% was measured using CO chemisorption.

Liquid-phase hydrogenation of C_4 olefins over 0.2 wt% Pd/Al_2O_3 spheres (2.34 mm in diameter) has shown to be accompanied by strong diffusion limitation at 40 °C [17]. This is also the case for liquid-phase hydrogenation of pyrolysis gasoline with commercial Pd/Al_2O_3 catalyst with a pore size distribution between 4 and 20 nm, even if an egg-shell catalyst is used for pygas hydrogenation [18, 19].

In the previous works the influence of preparation parameters on the properties of the resulting catalysts has been described. However, until now, there is no literature found considering the activity and stability of the catalysts under conditions relevant to industrial total hydrogenation process as well.

In this work, the effect of impregnation on the properties and performance of the Pd/Al_2O_3 catalyst in liquid-phase hydrogenation of C_3–C_4 olefins was studied. The effect of different preparation parameters such as HCl/$PdCl_2$ ratio, impregnation time and impregnation solution volume on Pd distribution and catalytic performance was investigated. Unlike many previous works, shaped supports were used and the catalytic performances in hydrogenation of light olefins were evaluated. The catalysts were characterized for properties by ICP, BET, XRD, NH_3-TPD and FESEM techniques. Performance tests were performed in a three-phase trickle bed reactor under typical industrial operation conditions.

Experimental

Catalyst preparation

Two γ-Al_2O_3 support samples (extrudate, 1.2 × 2–3 mm) were provided by Weifang (donated as WG) and Nano Pars Spadana (donated as SP) companies. The supports

were pretreated by calcining under dry air flow, using a heating rate of 5 °C min^{-1} and keeping at 450 °C for 3 h.

The catalysts were prepared by wet impregnation of the support with acidic solution of $PdCl_2$ (59%) to achieve the desired nominal loading of Pd. The support was first wetted by spraying water with volume equal to its pore volume (V_p). The impregnation solution was prepared by dissolving $PdCl_2$ with gradual addition of HCl (37%) with continuous stirring in a magnet-stirred beaker. The impregnation solution (V_p to $5V_p$) was added on the wetted support in a rotating balloon. After the specified impregnation time, the samples were filtered and the liquid was analyzed by UV–vis for residual Pd and Cl content. The samples were washed immediately three times with distilled water. Drying was performed at 110 °C overnight and calcinations at 450 °C for 3 h. A commercial catalyst (CatC) was used as the reference. Table 1 summarizes the operating conditions employed in catalyst preparations.

Catalyst characterization

Nitrogen adsorption/desorption measurements were carried out using a NOVA Quantachrome 2200 High-Speed Gas Sorption Analyzer, version 7.11. Before analysis, the samples were pre-treated under N_2 gas flow at 150 °C for 1.5 h. The isotherms were recorded at − 196 °C. The BET surface area was calculated from multi-point adsorption data in the relative pressure interval from 0.05 to 0.25.

Table 1 Catalyst samples preparation conditions

Sample	Support	Pd nominal loading (wt%)	V_{imp}/V_p	Cl_{HCl}/Pd (mol mol^{-1})	Impregnation time, t_{imp} (min)
Cat1	WG	0.9	1.3	0.117	20
Cat2	WG	0.6	5	4.20	180
Cat3	WG	0.6	1	4.20	180
Cat4	WG	0.6	2	1.99	20
Cat5	WG	0.6	1.3	0.176	15
Cat6	WG	0.5	2	8.50	10
Cat7	WG	0.5	5	7.66	105
Cat8	WG	0.5	2	5.96	60
Cat9	WG	0.5	5	5.96	60
Cat10	WG	0.5	2	5.11	20
Cat11	WG	0.5	5	2.50	180
Cat12	WG	0.5	2	2.38	20
Cat13	WG	0.5	2	0.85	20
Cat14	WG	0.5	1.3	0.212	5
Cat15	SP	0.5	5	5.110	20
Cat16	SP	0.5	5	2.50	180
Cat17	SP	0.5	2	2.38	20
Cat18	SP	0.5	1.3	0.212	5

The total micropore and mesopore volume (V_p) was determined using the t-plot method. The pore size distribution of the catalysts was determined by the BJH model applied to the desorption branch of the isotherms.

The XRD patterns of Al_2O_3 supports and the catalysts were recorded for phase identification using a Philips X-ray diffractometer model: X'Expert MPD (tube: Cu Kα radiation, voltage = 40 kV, current = 30 mA, wave lengths = λ_1: 1.54056, λ_2: 1.54439 and step size = 0.02°).

The metal penetration depth was analyzed by field emission scanning electron microscopy (FESEM) using a MIRA3 TESCAN-XMU apparatus. EDS analysis can be used to determine the elemental composition of individual points, line scans and to map out the lateral distribution of elements from the imaged area. To prepare the sample, a cross section of the extrudate catalyst was polished and covered with a Au layer and studied with the scanning electron microscope. The measurement was carried out under high vacuum by an electron beam with a voltage of 15 kV. In this work, the cross section (1.2 mm diameter) of the catalysts was divided into 40 points along the diameter. The percentage by weight of palladium and chloride at each point was measured within bulks with 50 nm dimension, given by the operator. The reported number is the average weight percentage of palladium and chlorine in each bulk.

The acidity of the supports and catalysts were characterized by ammonia temperature-programmed desorption (NH_3-TPD) with a conventional flow apparatus (BELCAT-A, BEL Japan, Inc.). A 35-mg sample was loaded in the U-tube. Before adsorption, the samples were initially degassed under He flow at 300 °C for 2 h at a heating rate of 10 °C min^{-1}. After cooling to 60 °C, the sample was saturated with ammonia for 1 h. After saturation, the sample was purged with helium for 30 min to remove the physically adsorbed ammonia on the surface of the catalyst. The temperature of the sample was then raised at a heating rate of 5 °C min^{-1} from 35 to 850 °C. The amount of ammonia desorbed from the catalyst was measured by comparing the TPD areas with that for a standard sample using a thermal conductivity detector (TCD).

The palladium content of the catalysts was measured by inductively coupled plasma (ICP; ICP-OES simultaneous instrument, model VISTA-PRO, Varian Inc.) from the diluted extract in aqua regia ($HCl/HNO_3 = 3/1$).

To assess the dispersion and average particle size of Pd on catalyst samples, CO-chemisorption test was performed. The samples were first reduced under H_2 gas (50 ml min^{-1}) up to 400 °C for 15 min in a glass reactor. Then, by connecting the reactor to the chemisorption apparatus (BELCAT, type A), and using a He flow of 50 mL min^{-1}, the reactor temperature was cooled down to 50 °C. Pulses of 1.009 mL CO (frequency, 1 per min) were introduced to the reactor and detected in the output stream by a TCD. The CO/He gas concentration was 10.0%. The observed stoichiometry of CO was considered one per atom of palladium [20].

Analyses by UV–vis spectroscopy were carried out on impregnating solutions to identify the residual palladium on filtered solution after impregnation. The analyses were performed by using a T90 + UV/vis Spectrometer PG Instrument Ltd.

Reaction study

Catalytic performance tests were carried out in an in-house made trickle-bed reactor (id = 1.0 cm). The mixed-phase feed (H_2 + hydrocarbon) enters through the top of the reactor and travels downward. To achieve good mixing and distribution of the feed, it was passed through a bed of inert material (quartz, mesh size 16) before entering the catalyst bed. The typical reaction condition was $T = 50$ °C, $P = 27$ bar and LHSV = 37 h^{-1} corresponding to commercial plant operation. The catalyst was reduced in situ with H_2 stream at 150 °C and 1 bar for 48 h prior to the hydrogenation experiment. The C_4 feedstock from complete saturation process (CSP) of a commercial plant (Table 2) was used as the feed. The product was analyzed with an online GC instrument Dani, Master Fast RGA Analyzer. The total olefin conversion was calculated from Eq. 4:

$$\text{olefin conversion} = \frac{\text{moles of olefins in feed} - \text{moles of olefins in product}}{\text{moles of olefins in feed}} \times 100 \quad (4)$$

The molar composition of olefins in the feed used in conversion calculation was based on the GC analysis results in Table 2.

Results and discussion

Characterization results

Figure 1 shows the Pd contents of the catalyst samples from ICP measurements. The metal loadings were very close to the corresponding nominal values given in Table 1 illustrating nearly complete uptake of the Pd precursor from impregnation

Table 2 Analysis of hydrocarbon feed

Component	Plant data (mol%)	GC test result (mol%)
H_2	0.037	–
i-C_4H_{10}	95.548	95.82
n-C_4H_{10}	0.702	0.69
Propane	0.455	0.39
i-C_4H_8	2.565	2.43
1-Butene	0.203	0.202
cis-2-Butene	0.173	0.182
trans-2-Butene	0.238	0.224
1,3-Butadiene	0.039	0003
Propylene	0.04	0.059
Total	100	100

solution by the supports under preparation conditions employed which is due to strong adsorption of the precursor by the support.

Figure 2 shows the time-dependent Pd uptake from impregnation solution for Cat15 catalyst as typical example. The maximum adsorption was reached in less than 5 min with adsorption above 93%, indicating rapid adsorption rates and high Pd-support interaction. Figures 1 and 2, respectively, illustrate that $PdCl_2$ adsorption on γ-Al_2O_3 is characterized by a high equilibrium constant and rate constant. This implies that uneven radial distributions of the adsorbates could occur because of diffusion limitation. However, within the pellet, equilibrium distribution could occur in longer adsorption times [13].

Figure 3 shows the XRD pattern of pretreated supports and some catalyst samples. They showed the three characteristic main peaks of γ-Al_2O_3 at 2θ of 37°, 46° and 66.5° confirming the predominance of γ-Al_2O_3 phase in the supports after calcination pretreatment. No characteristic diffraction peaks corresponding to Pd species were observed, which could be due to the low Pd loadings ($\leq$0.9 wt%) and/or high dispersion of the species [21]. The higher intensity of the peaks for WG support compared to SP implies higher crystallinity of the former. Furthermore, the full width at half maximum (FWHM) of the most intense diffraction peak (66.5°) of both supports was nearly the same (2.6°), implying similar crystallite sizes (ca. 3.7 nm) according to the Debye–Scherrer equation. It is worth noting that the seemingly lower crystallinity of Pd-impregnated samples (Cat1 and Cat14) compared to the support (WG) could be partly due to absorption of X-ray by the metal the extent of which depends on absorption coefficient and loading of the metal [22].

Table 3 shows the structural properties of the commercial catalyst (CatC), supports and prepared catalysts from N_2 adsorption/desorption results. The catalysts exhibited a small decrease in surface area compared to the support, which is mostly due to acid attack on γ-Al_2O_3 support during impregnation [23]. The

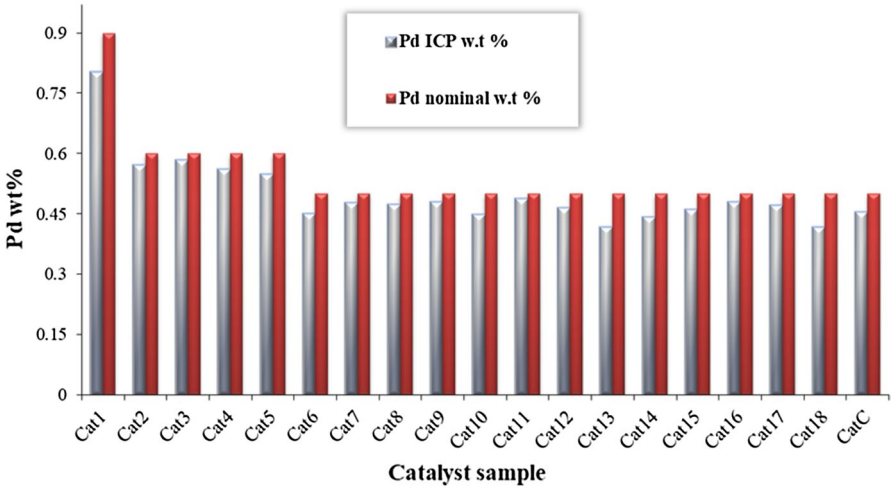

Fig. 1 Pd content of catalyst samples from ICP test results. (Color figure online)

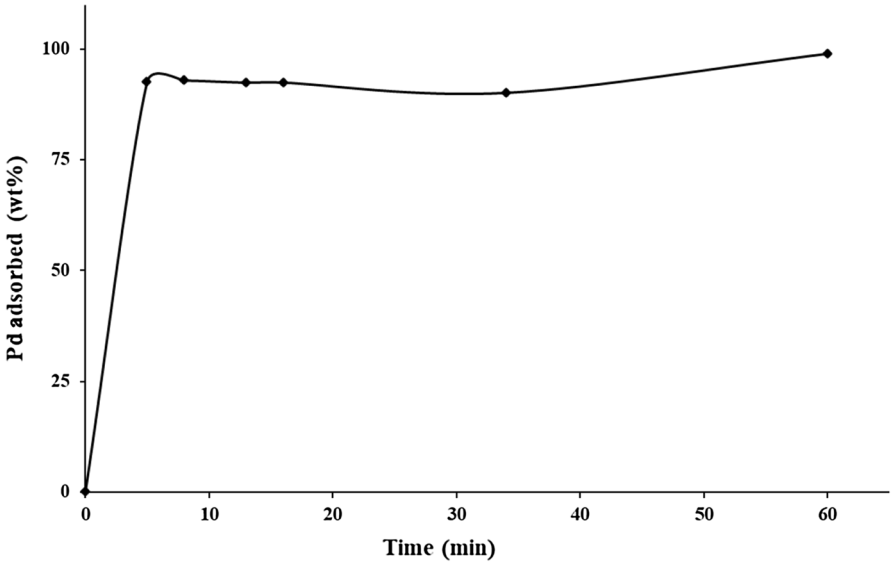

Fig. 2 Pd adsorption versus time for sample Cat15

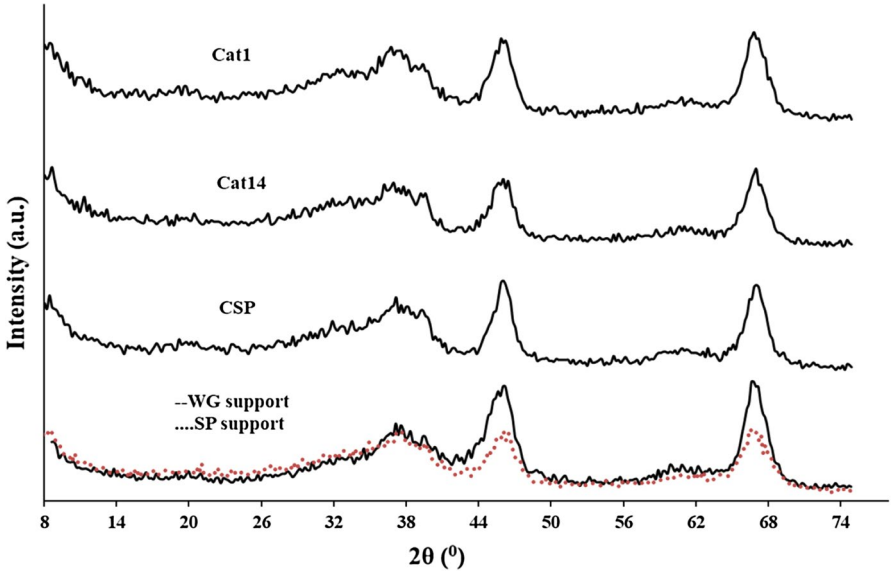

Fig. 3 XRD patterns Al_2O_3 supports and Pd/Al_2O_3 catalysts. (Color figure online)

solubility of γ-alumina in water becomes appreciable at a pH below about 3.5 [24]. However, the hypothesis has been advanced that acid attack on alumina is necessary for the adsorption process to occur [25].

The supports and catalyst samples showed narrow unimodal pore diameter distributions (not presented here) as obtained by applying the BJH method. According to the IUPAC classification [26], the internal pores of the catalyst are within the mesopore range (2–50 nm). The average pore diameters (10–13 nm) were much larger than the kinetic diameter of the C_4 hydrocarbon reactants and products (0.5–0.6 nm), implying no steric hindrance of pores for reacting molecules.

Figure 4 depicts the NH_3-TPD profiles of WG support and some WG-based samples. The WG support (Fig. 4a) exhibited three desorption peaks corresponding to weak (120–300 °C), medium (300–500 °C) and strong (500–650 °C) acid sites. The prepared catalysts, on the other hand, showed one additional desorption peak in medium acidity peak range (Fig. 4b). To elucidate the origin of the additional peak, NH_3-TPD tests were performed on WG support treated with different concentrations of HCl (impregnation solution pH of 2.2 and 0.9, samples WG1 and WG2, respectively) for 1 h, followed by the same thermal treatments as the catalysts. The additional peak was also observed in these samples (WG2, Fig. 4c) illustrating the significant role of the competitor HCl on acidity of the product. A comparative plot of acidity of the samples with different stages of preparation is illustrated in Fig. 4d. One observes that acidity increases with concentration of HCl used and also with impregnation with $PdCl_2$ precursor. The weak acid site concentration was most strongly affected.

It has been found that the presence of chlorine could increase the acidity of the support [27]. Both $PdCl_2$ and HCl are Cl^- containing compounds by which chlorine is added to the support as active component which enhancing the acidic function of the catalysts.

The NH_3-TPD measurement results also revealed that SP support showed much higher acidity (2.21 mmol g^{-1}) than WG support (1.05 mmol g^{-1}).

Figure 5 shows the FESEM profiles of Pd and Cl inside the selected catalysts pellets along with light microscope images of their cross section cuts. The catalysts were prepared with different impregnation times and pH, as they were considered the most effective parameters on active metal dispersion. The catalysts prepared with long impregnation times (Cat3, $t_{imp}=180$ min) and/or low pH values (pH 0.7, high competitor amount,; e.g. Cat6 and Cat7, respectively) exhibited relatively uniform profiles,

Table 3 Structural properties of the supports, commercial and some synthesized catalysts

Sample	Surface area (m^2 g^{-1})	Pore volume (ml g^{-1})	Pore radius (Å)
CatC	227.8	0.646	56.69
WG	212.6	0.68	64.03
Cat1	193.3	0.632	65.43
Cat5	199.8	0.66	66.08
Cat7	199.8	0.65	65.02
Cat14	182.7	0.63	68.79
SP	286.3	0.727	50.75
Cat18	256.2	0.677	52.86
Cat18 (spent)	253.0	0.659	52.08

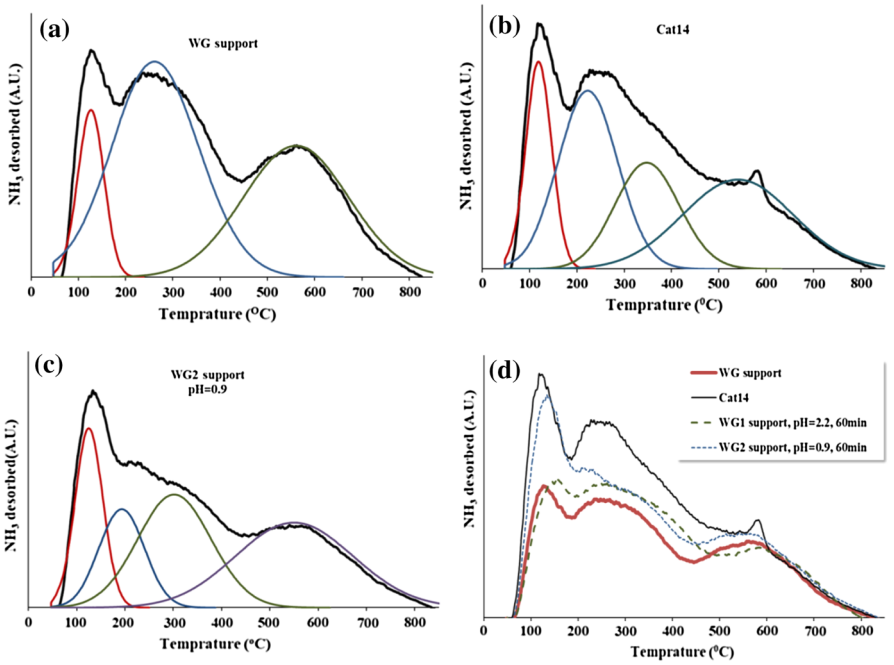

Fig. 4 NH_3-TPD deconvoluted profiles of **a** WG alumina support, **b** Cat14 sample, **c** WG treated with HCl solution with pH 0.9 and **d** comparative plot. (Color figure online)

which could be due to re-dispersion of the adsorbed species and competition effects, respectively. In the impregnation solution with lower acidity (pH 1.2) the distribution of Pd was shifted towards egg-shell type, when the impregnation time was shortened as long as other factors were kept constant (comparing Cat2 at $t_{imp}=180$ min with Cat4 at $t_{imp}=20$ min). In cases of short impregnation times and/or low competitor concentration (pH 2.2), the catalysts exhibited egg-shell type distribution of both adsorbed specie,s which is due to low intrapellet diffusion rates compared to adsorption rate (Cat14, Cat18 and Cat5).

As the FESEM profile shows the Cl was not completely removed by calcination and it located next to active sites. It is noteworthy that the high Cl/Pd ratio in Cat18 can be attributed to the high Cl content in the SP support.

According to the stability constant of palladium complexes, palladium was present mainly as $PdCl_4^{2-}$ in bulk solution [14]. However, when Pd chloride complexes contact the alumina surface, they undergo alkaline hydrolysis and they become $PdCl_2(OH)_2^{2-}$ because the surface (represented as Al–OH) acts as an alkaline medium due to its higher point of zero charge (PZC) compared to the solution pH. The hydroxyl groups of alumina surface show different acid–base properties. The basic OH (Al_B–OH) groups of the alumina surface will become more easily protonated in an acidic medium, as presented in Eq. 5 [28]:

$$PdCl_4^{2-} + 4Al_B{-}OH + 2H_2O \Leftrightarrow PdCl_2(OH)_2^{2-} + 4Al_B{-}OH_2^{+} + 2Cl^{-} \quad (5)$$

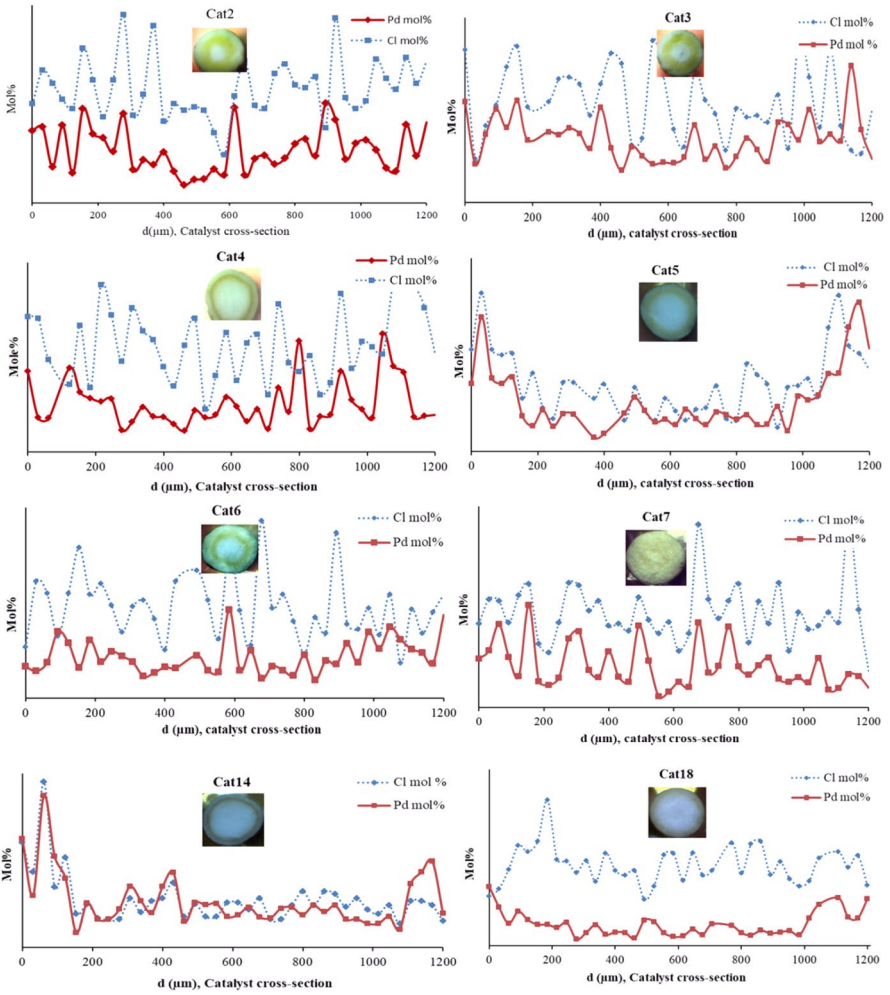

Fig. 5 FESEM profile of Pd and Cl in catalyst pellets. (Color figure online)

For short impregnation times (5–10 min) egg-shell profile is obtained especially for low concentrations of HCl. This is due to diffusion limitation for Pd precursors inside the pellet. At higher HCl concentrations, the interaction of Cl^- competitor with a higher concentration with the more positively charged alumina surface is preferential and $PdCl_2(OH)_2^{2-}$ complexes can move forward in the support body while Cl^- is retained in the outer edge occupying most of the adsorption sites in that area. This allows penetration of Pd towards the core at sufficiently longer time resulting in a variety of Pd distributions.

Within the pellet, the solution in the pores becomes more basic towards the core due to protonating the alumina surface. During diffusing into the pellet, the Pd chloride complexes hydrolyze as a consequence of the increase in pH of the solution towards

the core. The $PdCl_2(OH)_2^{2-}$ complex formed inside the pores of the support is still negatively charged also interacts electrostatically with the positively charged alumina surface. There are no electrostatic interactions between $PdCl_2(OH)_2^{2-}$ and the alumina surface because the adsorption sites of alumina in the edges of the pellet are occupied by Cl^- and $PdCl_2(OH)_2^{2-}$ (or other $PdCl_{4-x}(OH)_x^{2-}$ species) can move deeper within the catalyst body creating an egg-white or uniform distribution at longer times on stream for high $PdCl_{4-x}(OH)_x^{2-}$ species and low competitor concentrations, respectively [13].

It should be noted that the concentration profiles achieved during impregnation are retained during the subsequent preparation steps, namely, drying and calcination because of the strong interactions between Pd species and the alumina. However, after drying, chlorinated Pd is regenerated and retained after calcination.

Performance test results

Figure 6 shows the catalytic test results of the reference and some prepared catalyst samples. The olefin conversion declined steadily with time-on-stream over all catalyst samples as a result of catalyst deactivation. The catalysts exhibited a wide range of activity and stability.

For quantitative comparison of catalyst performances, the kinetic parameters for the main reaction and catalyst deactivation rate are necessary. A simple yet reasonable model for predicting deactivation and lifetime of a catalyst is

$$\frac{dA}{dt} = -k_d A^n \tag{6}$$

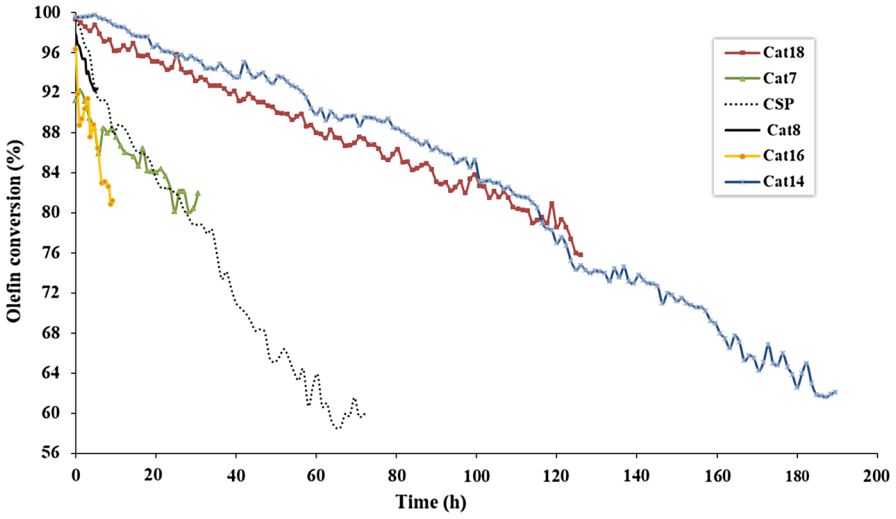

Fig. 6 Total olefin conversion versus time-on-stream over catalyst samples ($T = 50$ °C, $P = 27$ bar and LHSV = 37 h^{-1}). (Color figure online)

where A is activity, t time, n a constants that depends on process condition and mechanism and k_d is a deactivation rate constant [29]. For comparing different catalysts conveniently, it is advisable to fix n. Thus, for $n=1$ integration yields

$$A = A_0 \exp(-k_d t) \tag{7}$$

where A_0 is the initial activity. A_0 and k_d can be used as measures for the activity and stability of catalyst samples, respectively. A larger A_0 implies a higher activity while a larger k_d corresponds to a lower stability.

The stability trend of the catalysts versus their activity as indicated by deactivation rate constants and time-zero conversions, respectively, is illustrated in Fig. 7, in which the catalysts are sorted according to their activity. It shows that stability typically correlates inversely with activity. The increase of catalyst lifetime with its activity can be explained by the presumed parallel deactivation mechanism (Scheme 1). Upon increasing catalyst activity, the concentration of olefinic compounds which are coke precursors decreases within the reactor due to their hydrogenation to paraffins, thereby coke formation and deactivation rate decreases.

This result has an important practical implication for developing catalyst formulation since it relates stability and activity. Consequently, activity is the most important factor to be enhanced during catalyst development for complete saturation process. The stability, the other important property, would automatically improve.

The exceptionally low satiability of Cat16 could be correlated with the low pH of impregnation solution and higher acidity of the support used in its preparation both of which increase the acidity of the catalyst which promotes side reactions including coke formation. The chlorine residues originating from the precursor compound and preparative process has found to result in inferior

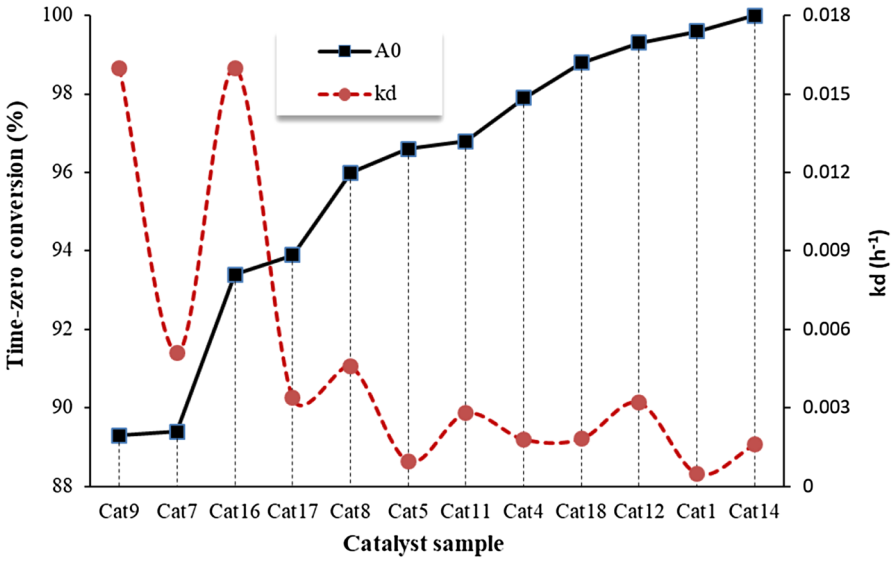

Fig. 7 Activity–stability comparison of different catalyst samples. (Color figure online)

catalytic performance which is thought to be associated with poisoning the hydrogenation process [30]. The lower activity of higher chlorine-containing supported palladium catalysts with a similar metal loading suggests that the chlorine is present at, or close to, those sites active for alkene hydrogenation. The reduced activity of the catalyst prepared from palladium(II) chloride with chlorine is attributed to a diminished hydrogen supply due to decoration of edge sites by chlorine originating from the preparative process [23].

A comparison of the catalysts prepared with WG and SP catalyst with the same recipe reveals that the catalyst prepared over the former exhibited superior properties. This could be attributed to the higher crystallinity and lower acidity of the former (e.g., Cat14 against Cat18). The NH_3-TPD results showed much higher acidity of Cat18 (2.52 mmol g^{-1}) compared to Cat14 (1.56 mmol g^{-1}) corresponding to those in the respective supports.

The activity of Pd/Al_2O_3 catalyst depends on metal loading and dispersion (collectively characterizing total surface metal atoms) and Pd distribution (characterizing availability of the active sites to reactants in diffusion-limited systems). The CO-chemisorption results showed that Pd dispersion ranged from 27% (Cat4 and Cat13) to 49% (Cat2). Interestingly, no clear relation was observed between catalyst activity and metal loading/dispersion, implying that distribution played more prominent role. This is consistent with strong diffusion-limitation in liquid-phase hydrogenation over Pd-based catalysts [17], limiting reaction to near-surface active sites. The Weisz–Prater criterion ($C_{WP} \sim 30 \gg 1$ for hydrogen in Cat 18) at reactor inlet confirmed significant diffusion limitations in the present work.

The optimum performance was observed for Cat14 prepared under high pH (low acidity) and short impregnation time. The catalyst showed egg-shell distribution of Pd. Because of the very low diffusivity of the reactants in liquid phase and high activity of Pd in hydrogenation reaction, the reaction is potentially intraparticle diffusion-limited [17–19]. Therefore, most of the reaction occurs in the outer zone of the catalyst pellet where most of the Pd is deposited in the case of egg-shell catalyst. This along with low acidity of impregnation solution can account for the desirable performance of Cat14.

The deactivation of porous catalysts by coke formation from side reactions is through active site coverage and pore blockage [31]. The parallel deactivation mechanism, as well as strong diffusion limitation favors the later for three-phase hydrogenation reaction over Pd-based catalysts. However, as shown in Table 3, only a small decrease in surface area, pore volume and pore diameter was observed for the spent Cat18 catalyst (after 126 h-on-stream) compared to the fresh one which could be attributed to coke deposition on the former. This implies that the main cause of catalyst deactivation was active site coverage by coke and pore blockage could not play a significant role. The relatively large pore size and pore volume of the supports, and thus catalysts, reduce the susceptibility of the catalysts to pore blockage unless severe coke formation occur.

Conclusions

The performance of Pd/Al_2O_3 catalysts prepared by impregnation in saturation of olefinic compounds strongly depends on preparation condition. The acidic solution of $PdCl_2$ is strongly adsorbed by γ-Al_2O_3 support. For a given Pd loading, the HCl/$PdCl_2$ ratio in impregnation solution and impregnation time is the most important parameters affecting active component distribution and acidity of the catalyst and, therefore, its catalytic performance. In addition, the alumina support with higher chlorine containing, lead to diminish of catalyst performance. Other preparation parameters such as impregnation solution volume are only of secondary importance. Low concentrations of the competitor and short impregnation times were found to be the suitable preparation conditions because they promote egg-shell type distribution of Pd which could be due to low intrapellet diffusion rates compared to adsorption rate which is the desirable one for the diffusion limited paraffin hydrogenation. It is noteworthy that the FESEM profile of Pd and Cl shows that Cl is not completely eliminated during calcination and it appears closely attached to the Pd active phase.

The stability of the catalysts showed a correlation with catalytic activity which is a consequence of parallel deactivation mechanism. Therefore, catalyst activity is the most important issue to be enhanced during catalyst development for CSP. The stability, the other important property, would automatically improve.

References

1. Á. Molnár, A. Sárkány, M. Varga, J. Mol. Catal. A Chem. **173**, 185 (2001)
2. F. Nierlich, F. Obenaus, Erdöl Kohle Erdgas Petrochem **39**(2), 73 (1986)
3. K.H. Walter, W. Droste, D. Maschmeyer, F. Nierlich, in *Selective Hydrogenations and Dehydrogenations, Proceedings of DGMK Conference*, *Kassel*, ed. by M. Baerns, J. Weitkamp (1993) pp. 31–48
4. G.A. Olah, Á. Molnár, G.K.S. Parkash, *Hydrocarbon Chemistry*, 3rd edn. (Wiley, New York, 2018)
5. M. Takht Ravanchi, S. Sahebdelfar, *Palladium as a Catalyst for Selective Hydrogenation: Fundamentals and Applications* (Lap Lambert Academic Publishing, Berlin, 2015)
6. G.C. Bond, *Metal-Catalyzed Reactions of Hydrocarbons* (Springer, New York, 2005)
7. B. Wang, G.F. Froment, Ind. Eng. Chem. Res. **44**(26), 9860 (2005)
8. O. Levenspiel, *Chemical Reaction Engineering*, 3rd edn. (Wiley, New York, 1999)
9. J. Panpranot, O. Tangjitwattakorn, P. Praserthdam, J.G. Goodwin Jr., Appl. Catal. A Gen. **292**, 322 (2005)
10. M.L. Toebes, J.A. van Dillen, K.P. de Jong, J. Mol. Catal. A Chem. **173**, 75 (2001)
11. O.B. Belskaya, T.I. Gulyaeva, A.B. Arbuzov, V.K. Duplyakin, V.A. Likholobov, Kinet. Catal. **51**(1), 105 (2010)
12. C.D. Tait, D.J. Janecky, P.S.Z. Rogers, Geochim. Cosmochim. Acta **55**, 1253 (1991)
13. L. Espinosa-Alonso, K.P. de Jong, B.M. Weckhuysen, Phys. Chem. Chem. Phys. **12**, 97 (2010)
14. C. Contescu, M.I. Vass, Letter **43**(2), 393 (1991)
15. C. Contescu, M.I. Vass, Appl. Catal. **33**, 259 (1987)
16. D. Łomot, W. Juszczyk, A. Karpiński, Appl. Catal. A Gen. **155**, 99 (1997)
17. N.O. Ardiaca, S.P. Bressa, J.A. Alves, O.M. Martinez, G.F. Barreto, Catal. Today **64**(3–4), 205 (2001)
18. Z. Zhou, T. Zeng, Z. Cheng, W. Yuan, Chem. Eng. Sci. **65**, 1832 (2010)
19. Z. Zhou, T. Zeng, Z. Cheng, W. Yuan, Ind. Eng. Chem. Res. **49**, 11112 (2010)
20. S. Komhom, O. Mekasuwandumrong, P. Praserthdam, J. Panpranot, Catal. Commun. **10**(1), 86 (2008)

21. P. Castano, B. Pawelec, J.L.C. Fierro, J.M. Arandes, J. Bilbao, Fuel **86**(15), 2262 (2007)
22. Z.Y. Zakaria, J. Linnekoski, N.A.S. Amin, Chem. Eng. J. **207–208**, 803 (2012)
23. T. Lear, R. Marshall, J.A. Lopez-Sanchez, S.D. Jackson, T.M. Klapötke, M. Bäumer, G. Rupprechter, H.-J. Freund, D. Lennona, J. Chem. Phys. **123**, 174706 (2005)
24. F. Tahriri Zangeneh, A. Taeb, K. Gholivand, S. Sahebdelfar, Appl. Surf. Sci. **357**, 172 (2015)
25. A.M. Shah, J.R. Regalbuto, Langmuir **10**, 500 (1994)
26. M. Thommes, K. Kaneko, A.V. Neimark, J.P. Olivier, F. Rodriguez-Reinoso, J. Rouquerol, K.S.W. Sing, Pure Appl. Chem. **87**(9–10), 1051 (2015)
27. Y. Zhang, Y. Zhou, H. Liu, L. Bo, M. Tang, Fuel. Process. Technol. **90**, 1524 (2009)
28. L. Espinosa-Alonso, K.P. de Jong, B.M. Weckhuysen, J. Phys. Chem. C **112**, 7201 (2008)
29. J.T. Richardson, *Principles of Catalyst Development* (Plenum Press, New York, 1989)
30. F.A. Gracia, J.T. Miller, A.J. Kropf, E.E. Wolf, J. Catal. **209**, 341 (2002)
31. C.H. Bartholomew, Appl. Catal. A Gen. **212**, 17 (2001)